Photo-microbial visible light-induced magnetic mass independent fractionation of mercury in a marine microalga

K. Kritee[1*#], Laura C. Motta[1], Joel D. Blum[2], Martin T. K. Tsui[3] and John R. Reinfelder[1]

[1] Department of Environmental Sciences, Rutgers University, 14 College Farm Road, New Brunswick, New Jersey 08901; [2] Department of Earth and Environmental Sciences, University of Michigan, 1100 N. University Avenue, Ann Arbor, Michigan 48109; [3] Department of Biology, University of North Carolina at Greensboro, 321 McIver St, Greensboro, North Carolina 27402

[*]To whom correspondence should be addressed; [#]Present address: Environmental Defense Fund, 2060 Broadway (Suite 300), Boulder CO 80303; Tel: (732) 277 8134 (Cell); Email: kriteek@gmail.com

Keywords: Mercury, Stable isotope, Mass independent fractionation, Mass independent fractionation, Intracellular MeHg degradation, Intracellular Hg(II) reduction, Radical pairs

Abstract

Methylmercury (MeHg), a highly neurotoxic substance, accumulates in aquatic food webs and is enriched in odd isotopes (i.e., ^{199}Hg and ^{201}Hg), purportedly as a result of abiotic photo-degradation in surface waters. Here, we highlight the potential role of phytoplankton in the mass independent fractionation (MIF) of MeHg in marine food-webs by providing evidence of 1) degradation of intracellular MeHg and reduction of intracellular inorganic mercury (Hg(II)) in the marine microalga, *Isochrysis galbana*; 2) a large, positive MIF ($\Delta^{199}Hg_{reactant}$ - $\Delta^{199}Hg_{product}$ ~5-10‰) during intracellular degradation of MeHg in cells exposed to visible light with no UVB, consistent with the accumulation of odd isotope-enriched MeHg in marine food-webs; and 3) a negative MIF (-1‰) during intracellular reduction of Hg(II) in the presence of UVB light. If representative of the photochemical reactivity of MeHg in marine phytoplankton, our results indicate that algal cell-mediated demethylation of MeHg by visible light could account for 20 to 55% of the total photochemically-driven demethylation in the open ocean and transparent freshwater ecosystems with deep euphotic zones. Thus, our results extend the importance of phytoplankton (and possibly other light permeable microorganisms) in mercury

biogeochemistry beyond their role as accumulators of MeHg and/or reducers of Hg(II) at the base of the food chain, to include MeHg degradation and MIF of Hg in sunlit layers of the ocean and other aquatic systems.

Introduction

Phytoplankton play an important role in the speciation, mobility, bioaccumulation, and toxicity of Hg in aquatic ecosystems[1-3]. Although Hg methylation in the marine water column has in some cases[4-6]been correlated with phytoplankton biomass or productivity or the seasonally variable growth of pico- and nanophytoplankton (as opposed to larger (>20 μm) cells)[7]; marine microalgae are not known to methylate Hg directly. They do, however, represent an important route for Hg entry into aquatic food webs[8, 9]. Methylmercury, which is the most biologically available organic form of Hg, is concentrated from the dissolved phase in phytoplankton by a factor of more than 10^4 from seawater[10, 11]. Cells enriched in MeHg are then consumed by zooplankton, which in turn are a primary food source of larval, juvenile, and some adult fish. Indeed, nearly all of the MeHg accumulated by zooplankton and fish is from their diet[12-14]. Two bacterial pathways that degrade MeHg, a reductive, enzyme-mediated process whose products are CH_4 and Hg(0), and (an) oxidative process(es) whose products are CO_2 and an unidentified form of inorganic Hg [ref 1 and references therein], have not been reported in phytoplankton. While the degradation of MeHg has been linked to the presence of plankton[15, 16], UV-mediated abiotic photochemical processes have been assumed to dominate MeHg degradation in the photic zone[15, 17], although the potential importance of dark microbial degradation of MeHg has also been discussed[18].

The reduction of Hg(II) in marine surface waters has been primarily attributed to two phenomena: abiotic photochemical reactions[19] (with photochemical reduction of Hg(II) being nearly balanced by photo-oxidation of Hg(0)[20]) and dark microbial reactions associated with Hg-resistant microorganisms[1]. However, it is not clear if these two phenomena can completely explain the reduction of inorganic Hg(II) observed in growing cultures of marine phytoplankton[21-24]. In addition, although direct positive relationships between Hg(0) concentrations and phytoplankton pigments have been observed in marine ecosystems[25], it is not clear if phytoplankton can directly and/or intracellularly demethylate

MeHg and/or reduce Hg(II) beyond their role in the production of extracellular dissolved organic matter (which may participate in abiotic photo-reduction). While Hg transformations within many different lineages of bacterial cells have been explored in detail, including the recent demonstration of the reduction of intracellular Hg in a photomixotrophic bacterium[24],, the role of photo-microbial transformations (intracellular photochemical reactions) of MeHg or Hg(II) within phytoplankton cells has not been specifically examined.

Mercury stable isotope fractionation has proven to be a useful tool in constraining the potential sources and transformations of different forms of Hg in the environment[26-28]. Mercury stable isotopes display both mass dependent fractionation (MDF) and mass independent fractionation (MIF). The magnetic moments of odd isotopes of Hg and the non-mass-dependent variation in the nuclear volumes of Hg isotopes, especially ^{199}Hg and ^{201}Hg[29-32], can lead to fractionation that does not scale according to isotope mass. While MDF has been observed during both dark transformations and photochemical reactions, MIF has not been observed during any dark microbial Hg transformations investigated to date[33-37].

With respect to stable isotope fractionation, photo-microbial Hg transformations lie at the interface between biology and photochemistry. Stable isotope fractionation of Hg during dark microbial reduction[33-35] and also during abiotic UV-mediated processes[29-31] has been documented, but the effects of intracellular photo-reduction/degradation of Hg(II) or MeHg in phytoplankton on Hg stable isotopes has not been explored[38]. A clear understanding of the Hg isotopic signatures of phytoplankton-mediated transformations, which could affect the isotopic composition of oceanic Hg(0) in addition to that of MeHg in fish, is necessary to interpret stable isotope ratios of Hg occurring as Hg(II) and MeHg both at the top of the food web (i.e., in fish) and in the water column and sediments.

We investigated the rates and Hg stable isotope signatures of photo-microbial transformations of Hg(II) and MeHg in marine phytoplankton exposed to visible light and varying levels of UV radiation by performing experiments with 1) sterile-filtered spent growth media containing extracellular exudates from cultures of *Isochrysis galbana,* a eukaryotic marine microalga of the globally important Prymnesiophyceae class ; 2) actively

growing mono-specific cultures of *I. galbana*; and 3) cysteine or ocean-water washed (non-growing) *I. galbana* cells. The washed cell experiments were designed to test the ability of phytoplankton to transform intracellular Hg(II) and MeHg. We present our results in the context of known reaction mechanisms and expected ligand interactions inside and outside of phytoplankton cells, and discuss the general implications of the new findings with respect to the current understanding of aquatic Hg biogeochemistry in the ocean and Hg isotope systematics.

Experimental Methods

Phytoplankton cultures: Experiments were conducted using the unicellular, eukaryotic, marine microalga *Isochrysis galbana* (strain ISO, CCMP1323). *Isochrysis*is a common genus in temperate marine waters and represents the globally distributed class *Prymnesiophyceae*. Live cultures of *I. galbana* were grown in Aquil artificial seawater media[39] with 300 μM nitrate and 10 μM phosphate and were maintained at 18°C under a 12:12 h light:dark regime with 200 μmol quanta m^{-2} s^{-1} irradiance provided by cool white fluorescent low pressure Hg lamps (see more below).

Mercury reduction experiments. Photochemical reduction of Hg(II) or MeHg was examined in growing whole culture, phytoplankton exudate, and washed cell experiments (see SI Tables 1 and 2 for details of all experiments). For all experiments, 100 μg/g inorganic Hg(II) and MeHg stocks were made from powdered Sigma Aldrich Mercuric Nitrate Monohydrate and powdered Crescent Chemical Company Methylmercury Chloride, respectively. For growing culture and exudate experiments, the Hg-free cultures were acclimatized to a 24 hour light regime for 2 days. After this acclimatization, cultures (or the collected spent media, i.e., culture filtered through 0.2 μm polycarbonate filters) were either incubated with Hg(II) or MeHg for up to 20 hours in the dark, after which, lights were turned on and reactors were purged with Hg-free air to start the reduction experiments. In growing culture experiments, both intra- and extracellular Hg was present and the kinetics and isotopic fractionation were affected by both algal exudates and the intracellular environment. For intracellular experiments, phytoplankton cells in the early exponential phase (between 4.5 x 10^4 and 5 x 10^4 cells ml^{-1}) were exposed to Hg(II) or MeHg at the beginning of a 12h

dark period and were allowed to accumulate Hg(II) or MeHg for up to 3 days. Repeated tests showed that, after this accumulation period, most of the added Hg(II) or MeHg was associated with the cells and the filtrate/exudate contained <2% of the added Hg. To remove extracellular Hg, cells were washed with a solution of reduced cysteine and/or synthetic ocean water (SOW) to removed surface-bound Hg[40-42]. Our data indicates that 30-40% of the Hg(II) associated with cells (in nmol/chla) after seawater wash is removed after cysteine wash (SI Table 1). As described earlier[42], the Hg that remains associated with cell surface after cysteine washing steps is not labile. In addition, the calculation of fractionation factor does not depend on the initial isotopic composition of the reactant Hg.

Briefly, to wash the cells, they were first concentrated by centrifugation (1600 x g, 3 min) and washed twice by re-suspension in 20 ml of SOW. For cysteine washes, the cells were re-centrifuged, and re-suspended in 20 mL of 8 mM cysteine for 4 min. The cysteine wash solution was prepared fresh just prior to use in N_2-purged 50% SOW. After being washed with cysteine, cells were washed with SOW and re-suspended in Aquil culture media without vitamins or trace metals. Stock phytoplankton cultures were initially axenic and all precautions were taken to exclude bacteria from experimental cultures.

All Hg reduction experiments were carried out in the laboratory at 22 to 25°C using cool white fluorescent lamps (Philips 48" 40 Watt F40T12/CWSUPREME/ALTO; see Supplementary information for details on energy emitted by the lamp and its effect on fractionation). Cells or exudates were incubated in either borosilicate glass (custom made at Univ. Mich.)[33] or UV transparent Nalgene Teflon® fluorinated ethylene propylene (FEP) 1 L, natural translucent narrow-mouth (381600-0032) bottles that were purged continuously with sterile (0.2 micron filtered) Hg free air to remove Hg(0) as described earlier[33]. The concentration and Hg isotopic composition of reactant Hg(II) or MeHg remaining in each reactor was tracked over time by periodically removing 50 mL samples which were immediately weighed and preserved in 0.2% HCl and 10% BrCl (w/w) as explained earlier[33]. Our work with microbial reduction of Hg(II) in same borosilicate reactors has shown previously that the results (i.e., fractionation factors) based on isotopic composition of the Hg remaining in the reactor *vs* isotopic composition of the vapor product trapped in $KMnO_4$

based oxidizing solution are similar even when there is some loss of Hg(0)[33]. Because of uncertainties involved in estimating 'f' as necessary for the Rayleigh distillation equation that is based on the vapor product as opposed to the liquid reactant remaining in the reactor, we did not trap the product Hg(0) (please see Kritee et al, 2007 and the associated supplementary material for more details). The usual $KMnO_4$ based traps do not maintain their oxidizing function over time periods longer than a few hours and our experiments ran for many days. Crucially, our previous work[33] has shown that irrespective of the efficiency of the $KMnO_4$ traps in trapping the product Hg(0), isotope data from trapped product (Hg[0]) showed no fractionation during volatilization/leakage of product from the apparatus.[33] For Teflon reactors, wall losses of Hg(II) and MeHg are not observed with seawater[43].

We used light meters for both visible (LI-COR LI-250 PAR light meter) and UV (Sper Scientific UV Light Meter UVA/UVB-850009) to measure adsorption spectra of the two kinds of reactors. The absorption spectra of the borosilicate and Teflon bottles show that similar levels of visible (73 to 79 μmol m^{-2} s^{-1}) and UVA (~5 μmol m^{-2} s^{-1}) light entered both kind of reactors (Table 1). However, only about 1/3 of the UVB that entered the Teflon bottles entered the glass bottles (Table 1). In some experiments with Teflon bottles, UV radiation was blocked using Lee 226 filters, which absorb 96-100% of light below 378 nm[15, 44] (Table 1). Thus in bottles with Lee filters, cells and exudates were exposed to very little (<0.01 μmol m^{-2} s^{-1}) UVB and less than 5% of the UVA in unshielded bottles (0.2 μmol m^{-2} s^{-1}).

The attenuation of light due to phytoplankton was estimated using measured light absorption of *I. galbana* cultures averaged over the wavelength ranges for UVB (280 to 300 nm), UVA (320 to 400 nm), and visible (400 to 700 nm) light. Culture absorbances were extended to the center of reactor Teflon bottles (5 cm) and converted to percent transmission. Based on these measurements, the average light attenuation due to phytoplankton was estimated as 25% of incident UVB, 20% of incident UVA, and 17% of incident visible light. For the custom-made borosilicate glass reactors which were in the shape of Erlenmeyer flasks, we estimated an average depth to center from the side and bottom of 6.5 cm (7.5 cm from the bottom, 5.5 cm from the side). For glass reactors, the

187 average attenuation of light due to phytoplankton was therefore 31% of incident UVB, 25%
188 of incident UVA, and 22% of incident visible light.
189
190 **Mercury concentration and isotope analysis:**
191 The total Hg concentrations were analyzed using a Nippon Instruments MA-2000 Hg
192 analyzer (Detection limit ~3.5 ppt and Quantification limit of <6 ppt) at the University of
193 Michigan. All samples were pre-treated and transferred to $KMnO_4$ matrix[45]; and standard
194 solutions of NIST-3133 were used for calibration curve. We also used an in house secondary
195 calibration standard for checking recoveries.
196 Mercury isotope ratios were also analyzed at the University of Michigan using a Nu
197 Instruments multiple collector inductively coupled plasma mass spectrometer (MC-ICP-MS)
198 according to our previously published protocols[46]. Nomenclature for Hg isotopic
199 compositions has been explained earlier[38]. Bracketing standards (NIST 3133) were diluted in
200 a neutralized $KMnO_4$-H_2SO_4 matrix and concentration matched within 5%. Blanks of the
201 same $KMnO_4$-H_2SO_4 solution were additionally employed to perform On-Peak-Zero
202 measurements before the standard and sample analysis and subtracted from the analyte
203 signals during data processing. Prior to introduction into the mass spectrometer, samples
204 were reduced online with 2% (w/w) tin chloride and Hg(0) was liberated from solution using
205 a custom built gas-liquid phase separator. Multiple preparations of UM-Almáden were used
206 to characterize instrumental performance (internal precision) (see SI Table 5). Replicate
207 analysis of our reactor samples could not be performed in this study because of much lower
208 concentration of Hg in the reactor and the need to reduce the entire sample for measurement
209 of one isotopic analysis on MC-ICP-MS. In general, replicate analysis of liquid samples in
210 $KMnO_4$ matrix after pre-treatment and secondary trapping had external precision (2SD) of
211 <0.1‰ for both $\Delta^{199}Hg$ and $\delta^{202}Hg$[45, 47].
212
213 Differences in isotopic composition between reactant and instantaneous product at
214 any given time during the course of a reaction were quantified as isotopic enrichment factors
215 (ε) in units of ‰. Isotopic enrichment caused by MDF ($\varepsilon^{202}Hg_{reactant/product}$) was quantified as
216 the slope of observed linear relationships between $\delta^{202}Hg_{reactant}$ and ln(f), where f is the
217 fraction of initial added Hg remaining in each incubation. Isotopic enrichment due to MIF

($\Delta^{199}Hg_{reactant} - \Delta^{199}Hg_{product}$) was quantified from the slope of Δ^{199}Hg-ln(f) relationships. Enrichment factors are related to fractionation factors ($\alpha = R_{reactant}/R_{product}$) by the relationship: ε (in units of ‰) = (α -1)*1000. The starting isotopic composition of our MeHg stock is lighter than the standards used during isotopic analysis but this does not impact the calculation of fractionation/enrichment factor. The presentation of Rayleigh plots and all subsequent calculations normalize for the starting isotopic composition of the reactant.

Results and Discussion

Kinetics of photo-microbial transformations of mercury Reduction/degradation of Hg(II) or MeHg by *I. galbana* cells in the dark was within experimental uncertainty for at least 16 hours (Figure 1A) and 28 hours (data not shown), respectively. In accordance with previous research that has demonstrated Hg(II) reduction in the presence of DOC and UVB radiation[29, 30], reduction of Hg(II) species in the presence of marine algal exudates, which consist of a complex mixture of DOC molecules[48-50], was observed with a very strong positive effect of UVB radiation on reduction rate of Hg(II) (first order rate constant (k) = 2.4 d^{-1} with high UVB *vs.* 0.06-0.10 d^{-1} with low UVB; SI Tables 1 and 3). A similar dependence of the rate of Hg reduction on UVB was seen in experiments with live and growing cells which included both extracellular as well as intracellular DOC and Hg(II) (k = 0.43 d^{-1} *vs.* 0.07 d^{-1}) or MeHg (k = 0.43 d^{-1} *vs*. 0.02 d^{-1}) in Teflon vs. borosilicate glass reactors (SI Tables 1 and 2).

Most importantly, we observed the direct reduction/degradation of intracellular Hg in the marine microalga *I. galbana* (SI Tables 1-4 and Figure 1). For the intracellular experiments, where cells were washed with cysteine (for Hg(II) exposures) or synthetic ocean-water (for MeHg exposures because MeHg is mostly intracellular in phytoplankton[9] and MeHg exposed cells were sensitive to cysteine), concentrations of Hg(II) and MeHg inside the *I. galbana* cells were 0.69 to 1.4 and 1.1 to 1.3 nmol per µg chlorophyll a, respectively (SI Tables 1 and 2). The reduction rate of intracellular Hg(II) (cysteine-washed cells) was 1.8 to 3-fold faster than that of Hg(II) in cells washed only with synthetic ocean-water (k = 0.15 to 0.21 d^{-1} vs. 0.38 to 0.47 d^{-1}) suggesting that surface-bound Hg(II) is not as

efficiently reduced as intracellular Hg(II) (SI Table 1). The degradation of intracellular MeHg (SI Table 2; k = 0.09 vs 0.14 day^{-1}) was slower than the reduction of intracellular Hg(II), but showed only a modest dependence on exposure to UVB light (Figure 1B).

Our intracellular experiments were carried out under low irradiances and with relatively high concentrations of Hg(II) and MeHg inside *I. galbana* cells (SI Tables 1 and 2) to capture the change in isotope composition of reactant Hg species at the lowest possible concentrations required for precise isotope analysis, as is necessary in experimental studies of Hg isotope fractionation during microbial and photochemical transformations[29, 38]. While the rate constants for photo-microbial intracellular Hg(II) reduction we observed (0.4 to 0.5 d^{-1}, SI Table 1) are much lower than those for photochemical reduction observed in coastal marine surface waters (4 to 58 d^{-1})[18, 44, 51], they are an order of magnitude greater than that reported for dark biotic reduction of Hg(II) (0.03)[21, 44]. In addition, our rate constants for the photo-microbial degradation of intracellular MeHg (0.09 to 0.14 d^{-1}, SI Table 2) are comparable to those for MeHg degradation in unfiltered estuarine and coastal marine waters (k = 0.09 to 0.4 d^{-1})[18] as well as that in a clear water lake (0.17 d^{-1}) with more than six times the visible light than in our experiments[15].

Mass dependent fractionation during transformations of intracellular Hg: Photochemical reduction of intracellular Hg(II) and MeHg resulted in positive MDF (higher δ^{202}Hg values in the reactant) indicating a preferential degradation/reduction of molecules containing lighter isotopes of Hg(II) or MeHg (SI Tables 3 and 4). Reduction of Hg(II) incubated in the light with cell exudates, but no cells, led to a higher isotopic enrichment ($\varepsilon^{202}Hg_{reactant/product}$, see Methods, hereafter ε^{202}Hg, of 1.1 to 1.5‰) compared to intracellular (ε^{202}Hg = 0.7 to 0.8 ‰) or growing algae experiments (ε^{202}Hg= 0.1 to 0.6‰) (SI Table 1). Reduction of Hg(II) bound to serine (N containing ligand) leads to higher MDF than Hg(II) bound to cysteine (S containing ligand)[31]; it is plausible that in intracellular and growing algae experiments, Hg(II) is primarily associated with thiol (-SH) groups that protect the cell from oxidative damage. However, in experiments with cellular exudates, many other non-sulfur ligands bind to Hg(II).

Intracellular degradation of MeHg caused significant MDF (ε^{202}Hg = 0.9 to 1.7‰) both with and without UV light (SI Figure 1 and SI Table 2). Whereas previous research showed that abiotic photo-degradation of MeHg in the presence of UV light resulted in a high extent of MDF (with ε^{202}Hg = 1.4 to 1.6‰)[29], in our experiments abiotic reduction of MeHg (with algal exudates or in filtered synthetic ocean-water) in the absence of UV radiation caused very little MDF (ε^{202}Hg < 0.1‰). The fact that abiotic demethylation controls under low UVB conditions did not show much MDF (or any MIF, see below) is likely because in absence of intracellular processes that are activated by PAR, low UVB treatments are not able to generate radical pairs necessary for magnetic isotope effect. Overall, in our study, the photo-microbial reduction of intracellular MeHg resulted in higher MDF than abiotic photochemical reduction of extracellular MeHg in the absence of UV light. There is no clear effect of kinetics since intracellular degradation of MeHg was slightly faster than the abiotic reaction (SI Table 2). While detailed studies of the mechanisms of intracellular and abiotic MeHg degradation are needed to explain this difference, it is clear that the transformation within live phytoplankton cells resulted in greater isotopic selectivity than the abiotic reactions.

For some MeHg experiments, temporal trends in the δ^{202}Hg of Hg remaining in the reactors was not linear when plotted as a Rayleigh distillation curve [ln R/R_0 vs ln (f)] even though changes in Δ^{199}Hg were linear (e.g., compare SI Figure 1 and Figure 3 for growing algae (low UVB); data in SI Table 4). We note that the remaining Hg analyzed for isotopic composition may have contained both Hg(II) and MeHg (the methodology for quantitatively separating Hg(II) and MeHg for isotopic analysis that is being used now[52] was not available at the time of these experiments). Therefore, the observed non-linearity of the MDF signal may have been caused by the formation of Hg(II) during MeHg degradation and MDF during both the conversion of MeHg to Hg(II) and of Hg(II) to Hg(0). Neither Hg(II) nor MeHg would adsorb to the reactor walls given the high concentration of chloride in seawater[43], and the presence of cell-surfaces and intracellular moieties that have high concentrations of –SH groups. Moreover, adsorption would not have caused the observed non-linear trends (SI Figure 1). In contrast, it is likely that MIF is caused by only a single step (MeHg to Hg(II); see below).

Please see supplementary text for more observations related to MDF during Hg(II) reduction and MeHg degradation.

Mass independent fractionation during intracellular Hg reduction: The photochemical reduction of Hg(II) by growing algae, algal exudates, and intracellular algal components led to negative MIF indicating preferential enrichment of odd-mass isotopes in the product pool (Figure 2, SI Tables 1 and 3). Of these three treatments, the highest isotopic enrichment due to MIF was observed during the photo-microbial reduction of intracellular Hg(II) ($\Delta^{199}Hg_{reactant} - \Delta^{199}Hg_{product}$ = -1.03 ‰).

In contrast to Hg(II) reduction, photo-microbial degradation of MeHg in incubations of growing whole phytoplankton cultures and washed cells (intracellular experiments) showed positive MIF of Hg isotopes resulting in the accumulation of ^{199}Hg in the reactant pool (Figure 3, SI Tables 2 and 4). Intracellular MeHg degradation resulted in very large extents of positive MIF (Figure 3), regardless of the levels of UV light (Table 1 and Figure 3). However, MeHg degradation during abiotic control experiments (with seawater and exudates), with low levels of UV light (see Table 1, algal spent media containing exudates and abiotic synthetic ocean water) did not cause any MIF likely because low UVB treatments are not able to generate radical pairs necessary for magnetic isotope effect. Crucially, the range of high, positive MIF observed during the photo-degradation of intracellular MeHg ($\Delta^{199}Hg_{reactant} - \Delta^{199}Hg_{product}$ = 5.6‰ to 9.8‰) overlaps with results from our growing culture experiments ($\Delta^{199}Hg_{reactant} - \Delta^{199}Hg_{product}$ = 3.5‰ to 8.3‰) as well as results previously reported for abiotic photo-degradation of MeHg in the presence of DOC ($\Delta^{199}Hg_{reactant} - \Delta^{199}Hg_{product}$ = 3.3 to 7.8‰)[29] (SI Table 2).

Mechanism of photo-microbial Hg reduction and fractionation: Our results suggest that the Hg isotopic fractionation of intracellular Hg(II) follows that of the photochemical reduction of Hg(II) bound to thiols. Both MDF (~0.75‰) and MIF (~ -1‰) signatures generated during the photochemical reduction of intracellular Hg(II) in *I. galbana* are closer to that observed for the reduction of cysteine-bound Hg(II) (MDF of 1.3‰ and MIF of -1‰)[31] than that produced during the abiotic photochemical reduction of Hg(II) bound to serine (MDF of 1.7‰ and MIF of 3‰) or other ligands[31]. Thus, our results suggest that

intracellular Hg(II) is largely complexed by thiols, which are abundant in phytoplankton cells[53-55] and that all prokaryotic and eukaryotic microbial cells containing Hg(II) are potential sources of ^{199}Hg and ^{201}Hg-enriched Hg(0) when exposed to UV light. Although we cannot identify the exact cause of the low extent of MIF of Hg(II) in the growing cells experiment, it is possible that a combination of positive and negative MIF contributed to the net isotope fractionation observed in this treatment, which contained Hg bound to exudates, cell surfaces, and intracellular ligands. It has been established that reduction of Hg(II) bound to ligands containing –SH groups causes negative MIF (enrichment of odd isotopes in product) and reduction of Hg(II) bound to N or O containing ligands causes positive MIF (enrichment of odd isotopes in remaining reactant)[31]. Regardless of the differences among treatments, net MIF in all experiments with Hg(II) was negative and the highest magnitude of negative MIF was observed during the reduction of Hg(II) in the "intracellular" treatment.

It seems likely that different reaction mechanisms drive photo-microbial reduction of intracellular Hg(II) and MeHg. Comparable Hg(II) reduction and MeHg degradation experiments carried out under similar growing cell conditions (similar cell densities and irradiances) in borosilicate glass reactors (i.e., with low UVB radiation, Table 1) show that while MeHg underwent reduction with positive MIF ($\Delta^{199}Hg_{reactant} - \Delta^{199}Hg_{product} = 3.5‰$), Hg(II) reduction in glass reactors resulted in very low negative MIF ($\Delta^{199}Hg_{reactant} - \Delta^{199}Hg_{product} = -0.08‰$). The very small extent of MIF during the reduction of Hg(II) in these experiments may have resulted from the low level of UVA and UVB or the speciation of intra- and/or extracellular Hg(II). Longer outdoor experiments are impractical but we note that abiotic outdoor experiments (in natural sunlight) with Hg(II) bound to cysteine did not lead to any Hg(II) reduction in the absence of UV light (Teflon + UV-B Lee filter) for ~11 hours (both starting and ending concentrations were 40 ppb).

Our results show large extents of positive MIF and low $\Delta^{199}Hg/\Delta^{201}Hg$ ratios (~1 for Hg(II), SI Figure 2; ~1.2 for MeHg, SI Figure 3), indicative of the magnetic isotope effect (MIE). We note that our data provide no support for MIF due to UV self-shielding (SI Tables 3-4 and SI Figure 2) or nuclear volume effect. Large extents of MIF, that occur during abiotic photochemical transformations of Hg(II) and MeHg bound to organic ligands with O, N or S

functional groups, have been ascribed to the magnetic isotope effect (MIE)[29, 31] which leads to a $\Delta^{199}Hg/\Delta^{201}Hg$ ratio of 1.0 for Hg(II) and 1.2 to 1.3 for MeHg, which is in contrast to a higher value of 1.6 for the nuclear volume effect[32]. The pathway leading to this magnetic MIF has been proposed to be UV driven generation of radical pairs, which leads to spin inter-conversion mediated by hyperfine coupling. Our results (see SI Figures 2-3) support the conclusion that the fundamental pathway responsible for MIF in our experiments is magnetic MIF.

Possible routes for generation of radical pairs: The pathway leading to MIE during abiotic photochemical reactions (e.g., Bergquist & Blum, 2007) has been proposed to be UV driven generation of radical pairs (which leads to spin inter-conversion mediated by hyperfine coupling)[29, 31]. To the best of our current understanding, generation of radical pairs is necessary for magnetic isotope effect. While the exact pathway to generation of radical pairs in our intracellular demethylation experiments is not clear at this time (see two options below), involvement of MIE during the photo-microbial reduction of intracellular MeHg provides evidence for the generation of radical pairs in the presence of visible light and very low intensities of UVA (i.e,, in absence of significant UV). We can not rule out extra-cellular demethylation of MeHg (that remains associated with cell surface after seawater wash[56]). However, given the seawater vs. intracellular environment, we expect intracellular (soluble) MeHg to be more reactive than membrane-bound MeHg.

So how are these radical pairs generated inside cells? Singlet oxygen has been shown to be the likely reductant in the UV-mediated abiotic demethylation of MeHg[57]. While the photosynthetic apparatus of algae can generate singlet oxygen with photosynthetically active radiation (PAR i.e., visible light) and without UV[58]; it is unclear if, or how, singlet oxygen can lead to generation of radical pairs which are necessary for MIE. Another possibility is that the intracellular radicals[59] and radical pairs[58] generated in phytoplankton cells due to oxidative damage lead to MIE.

Photo-microbial contribution to the MIF signature of Hg in fish and MeHg degradation in marine surface waters: Photo-microbial reduction of intracellular Hg(II) in the presence

of UV radiation, which produces negative MIF in the reactant pool (Figure 2, SI Tables 1 and 3), could not contribute to the positive MIF signature of Hg widely observed in fish[26, 28, 29]. Moreover, and in contrast to MeHg, Hg(II) accumulated by phytoplankton is poorly assimilated by grazers[9] and thus is not efficiently transferred to fish (Hall et al., 1997). Experimental caveats notwithstanding (see above), based on our rate constants for the photochemical reduction of intracellular Hg(II) scaled to 12 hours of daylight (~0.2 d^{-1}), the average concentration of inorganic Hg(II) in suspended particles in the ocean (40 fM)[20], and assuming that 9% of particulate Hg(II) is intracellular[9], we estimate that photo-microbial reduction of intracellular Hg(II) could account for a global annual Hg reduction rate of ~5 Mmol y^{-1} (see SI Table 6 for calculations). This is of the same order of magnitude as the annual rate of biological reduction of Hg(II) in the mixed layer of the ocean (17 Mmol y^{-1}) and the vertical flux of Hg from the surface to deep sea by particle sinking (16 Mmol y^{-1}), as estimated by Soerensen et al[20]. While the net Hg isotopic fractionation associated with the much larger, but nearly balanced rates of abiotic photochemical reduction and oxidation of Hg (ca. 1000 Mmol y^{-1} each) is uncertain, the reduction of intracellular algal Hg(II) is expected to produce Hg(0) in marine surface waters that is enriched in ^{199}Hg in excess of its mass-dependent value.

In contrast to transformations of Hg(II), the photo-degradation of intracellular MeHg resulted in large extents of positive MIF in the reactant (Figure 3). Indeed, Δ^{199}Hg vs. δ^{202}Hg trajectories for the photo-microbial degradation of MeHg, with or without UVB light (see Table 1 for details of UV intensities), are similar to those for UV-driven, abiotic degradation of MeHg[29], and the isotopic compositions of the primarily MeHg in both freshwater[29] and oceanic[26, 27] fish (Figure 4). This result indicates that intracellular degradation of MeHg in phytoplankton, in the presence of visible light (with no UVB and very low UVA) could contribute to the accumulation of odd isotope-enriched MeHg in marine consumers. Since the soluble components of phytoplankton cells are preferentially passed on to zooplankton (algal cell walls are largely egested as fecal pellets[9]), and subsequently to organisms higher up in the food web, we expect the isotopic composition of soluble MeHg in phytoplankton will be transferred to higher trophic levels as well. As shown in Figure 4, marine consumers are enriched in odd isotopes of Hg. The relative contribution of extracellular (abiotic) vs. intracellular photochemical degradation of MeHg to the enrichment of odd mass isotopes of

Hg in marine consumers will depend on the environmental factors that control the percentage of total MeHg associated with plankton (e.g., microbial community composition and biomass, speciation of extracellular MeHg). We suggest that intracellular processes are expected to be most important to the enrichment of odd mass isotopes in marine food webs in ecosystems with high concentrations of phytoplankton (e.g., coastal or eutrophic ecosystems); however, this process may be important in high light, oligotrophic systems with deep chlorophyll maxima as well.

If representative of the photochemical reactivity of MeHg in marine phytoplankton generally, our results would extend the depth over which photo-degradation of MeHg in natural waters can occur and the potential influence of magnetic MIF on global aquatic Hg isotope geochemistry from the UV penetrable zone (typically limited to the top 1 to 5 m) to almost the entire photic zone. For example, applying a demethylation rate constant of 0.045 d^{-1} (for 12 hours of daylight), as determined for our intracellular, visible light-mediated (PAR = 63 μmol m^{-2} s^{-1}; Table 1, Teflon plus Lee, see Methods) algal demethylation experiment (SI Tables 2 and 4, Figure 3), to a phytoplankton MeHg concentration of 3 fM[17] from the sea surface to the 10% light level of the euphotic zone in the North Pacific Ocean (~54 m, average PAR ≈200 μmol m^{-2} s^{-1})[20, 60], yields a photo-demethylation rate of ~5 pmol MeHg m^{-2} d^{-1} (see all assumptions in SI Table 6). Based on rate constants for photochemical demethylation in marine surface waters scaled to 12 hours of daylight (0.04 to 0.2 d^{-1})[16, 18] and the concentration of dissolved MeHg in surface waters of the North Pacific[17], we estimate an abiotic, UV-dependent MeHg photo-demethylation rate of 4 to 20 pmol m^{-2} d^{-1} for the upper 5 m of the ocean. Algal cell-mediated demethylation of MeHg by visible light could therefore account for 20 to 55% of the total (due to both visible and UV light) photochemically-driven demethylation of MeHg in the open ocean and transparent freshwater ecosystems with deep euphotic zones**.** While further experiments are needed to evaluate the global applicability of the present results, if representative of the real ocean they would extend the importance of phytoplankton (and possibly other light permeable microorganisms) in mercury biogeochemistry beyond their role as accumulators of MeHg and/or reducers of Hg(II) at the base of the food chain, to include MeHg degradation and MIF of Hg in sunlit layers of the ocean and other aquatic systems.

Acknowledgements The authors would like to thank Tamar Barkay for her involvement in the conception of this project and comments on this manuscript, Sarah Janssen for help with experiments at Rutgers and Marcus Johnson for help with stable isotopic analysis at the University of Michigan. We also thank Laura Sherman and Sae Yun Kwon for insights on various aspects of this manuscript. Funding was provided by the NSF Geobiology and Low-Temperature Geochemistry program, EAR-0952291 to J.R.R. and EAR-0952108 to J.D.B, the NSF Chemical Oceanography program, OCE-1634154 to J.R.R., and a Hatch/McIntyre-Stennis grant through the New Jersey Agricultural Experiment Station.

Author contributions "K.K., L.C.M., J.D.B., and J.R.R. conceived and designed the experiments; K.K. and L.C.M. performed the experiments; M.T.K.T. and L.C.M. performed the MC-ICP-MS runs; K.K., L.C.M. and J.R.R. analyzed the data and prepared tables; J.D.B. contributed to the interpretation of results; K.K. and J.R.R. co-wrote the paper."

Supporting Information

Includes supplementary text, SI Tables 1-6, SI Figures 1-3 and SI references

484 **Table 1.** Light transmission (%T) and irradiances (E, μmol m^{-2} s^{-1}) in experimental bottles.

485 Values do not include light attenuation due to phytoplankton (see text).

486

	UVB (280-320 nm)		UVA (320-400 nm)		VIS (400-700 nm)	
Container	%T	E	%T	E	%T	E
Glass	24	0.9	84	5.0	91	73
Teflon	66	2.5	82	4.9	99	79
Teflon (Lee)	0.2	<0.01	4	0.2	79	63

487
488

489

490

Figure 1. "Photo-microbial" reduction of Hg in the marine microalga *Isochrysis galbana***.** Reduction of (A) intracellular inorganic Hg(II) in cells washed with cysteine and (B) intracellular methylmercury (MeHg) in cells washed with synthetic ocean water. For the Hg(II) experiment (1A), cells were incubated in the dark for the first 16 h before being exposed to UVB in a Teflon reactor. For the MeHg experiments, cells were incubated in 12:12 Light:Dark cycle followed by exposure to light in Teflon reactors with (no filter, red circles) and without (Lee filter, green circles) UVB (1B). Lines are best-fit models based on linear regression.

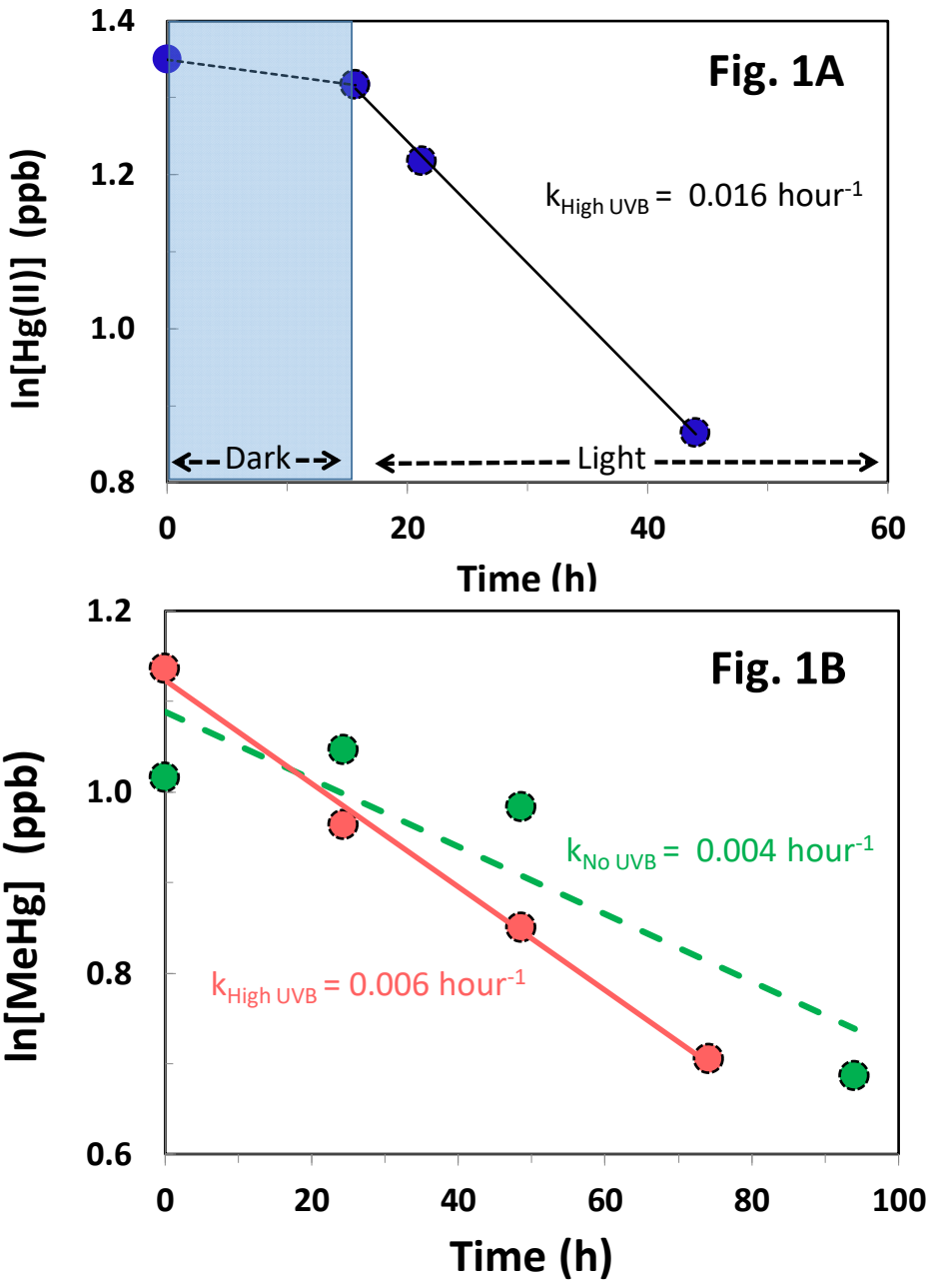

Figure 2. Negative mass independent fractionation during photo-microbial Hg(II) reduction by *Isochrysis galbana* in the presence of UV. MIF isotope enrichment factors calculated as the slopes of Δ^{199}Hg vs. ln(f) relationships are shown for three types of Hg(II) reduction experiments: growing algae (in brown), abiotic exudates (in green), and washed cells (intracellular, in blue). No Hg(II) reduction was observed in the absence of UV light. Δ^{199}Hg values plotted on the Y-axis have been corrected for the non-zero starting point.

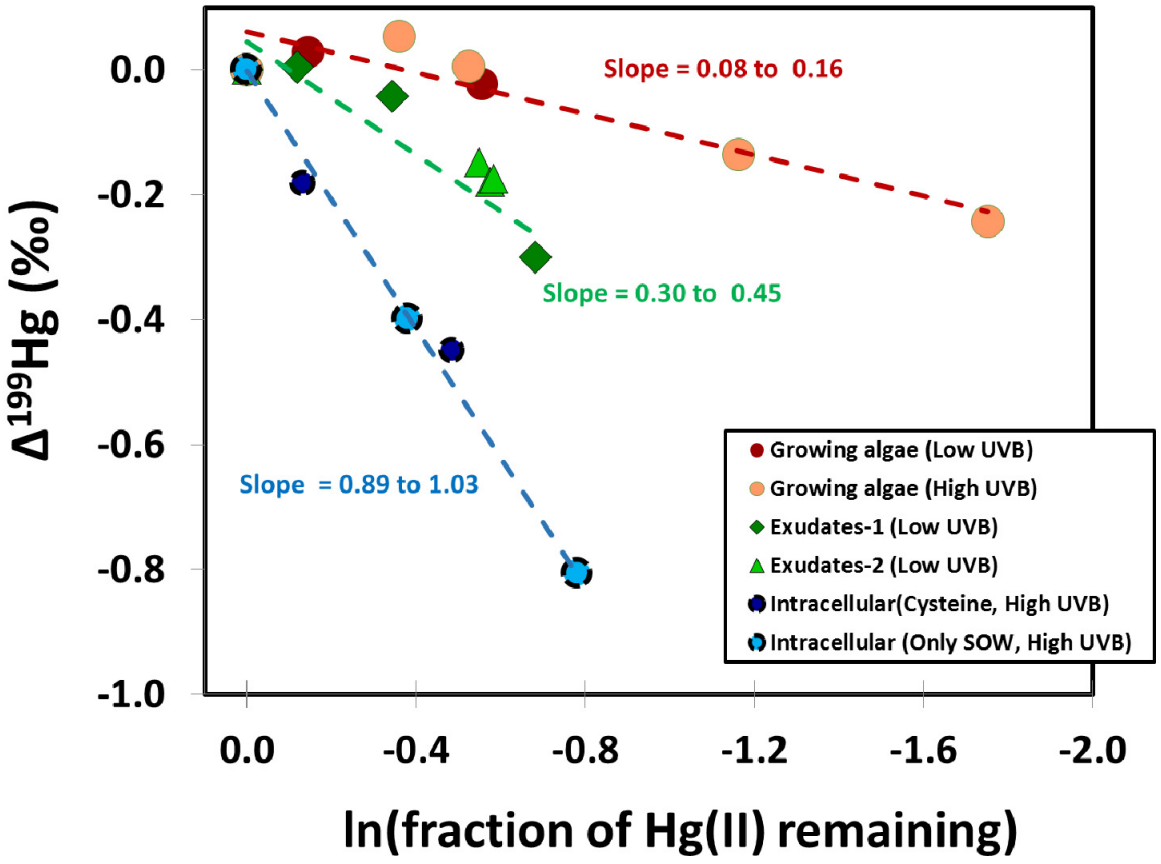

Figure 3. Mass independent fractionation during photo-microbial MeHg degradation by *Isochrysis galbana* in the presence of UV. MIF (Δ^{199}Hg vs. ln(f)) during MeHg degradation by algae (i.e., intracellular + growing cell experiments) under conditions of no UVB (in the presence of visible light and a very limited amount of UVA) is similar to MIF in the presence of high UVB. In contrast, abiotic controls (with no or low UVB) led to negligible MIF. The dotted lines represent the lower and upper 95% confidence intervals for photo-microbial reduction. Δ^{199}Hg values plotted on the Y-axis have been corrected for the non-zero starting point.

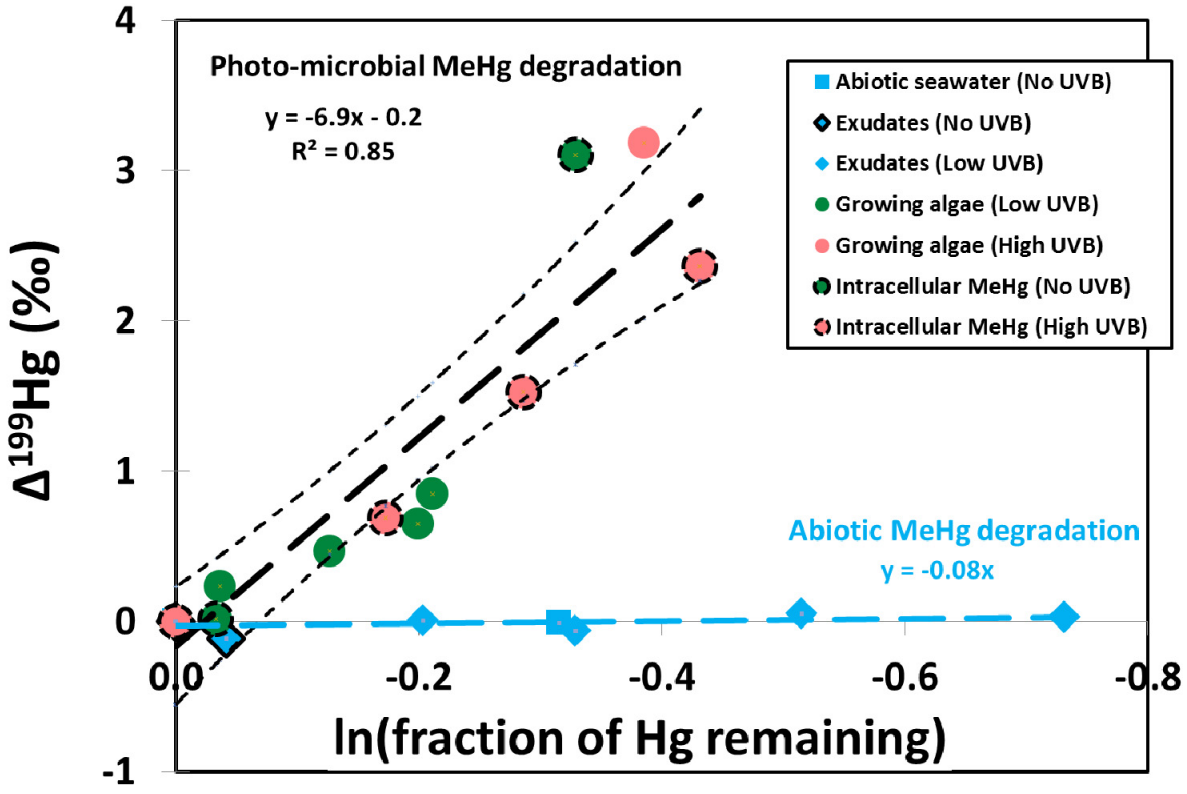

Figure 4 Mass independent (Δ^{199}Hg) and Mass dependent (δ^{202}Hg) signatures in fish *vs* fractionation during photo-chemical and photo-microbial processes. A comparison of marine[26, 27] and freshwater fish[29] isotopic data with stable isotopic fractionation during degradation of MeHg by photo-microbial (algal) and UV mediated photo-chemical processes[29] shows that photo-microbial processes could contribute towards the accumulation of odd isotope-enriched MeHg in marine consumers. The photo-microbial and photochemical regression lines are based on all four photo-microbial demethylation experiments reported in this figure and abiotic photochemical reduction with 10 mg C/L[29], respectively. The starting isotopic composition of MeHg stock used in our study is lighter than the standard used for isotopic analysis.

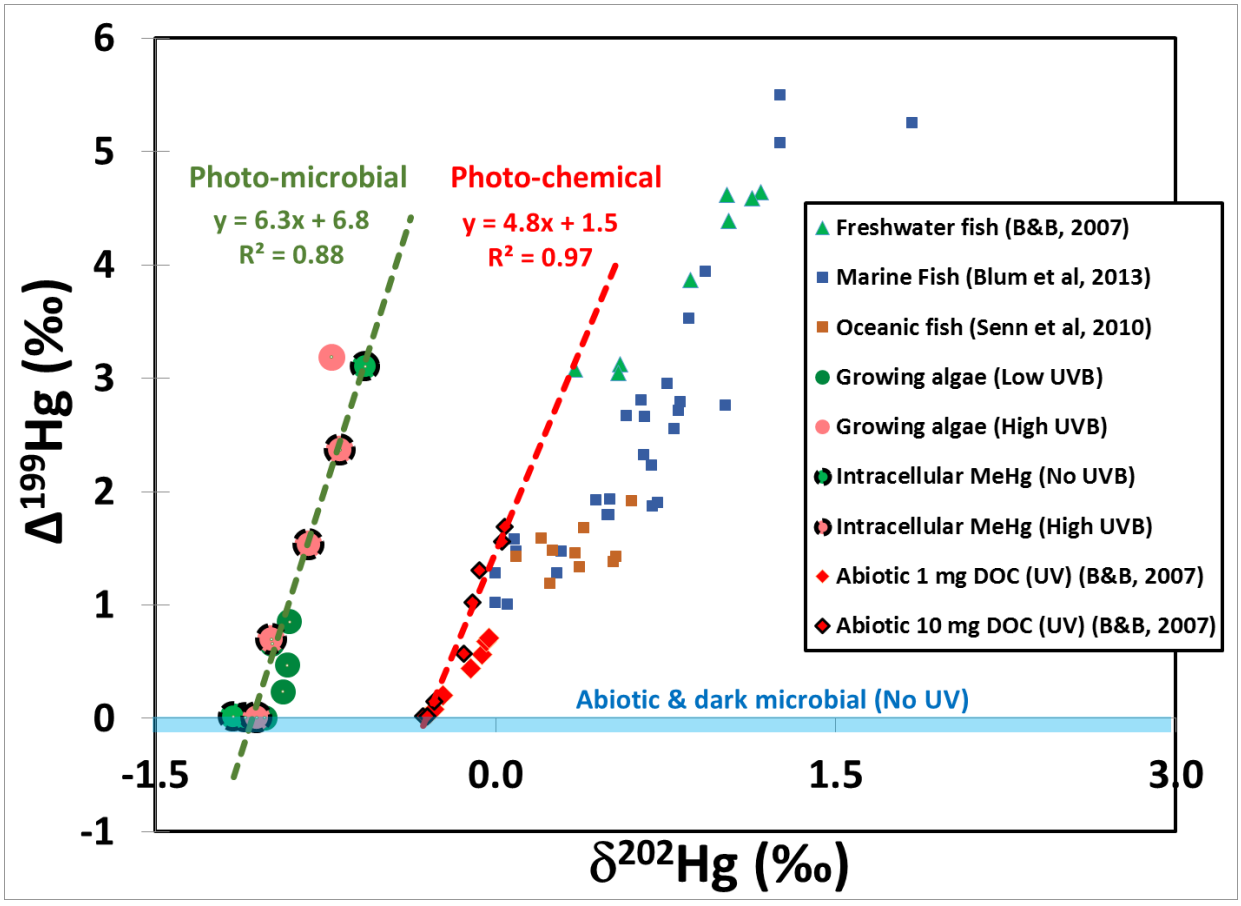

References

1. Lin, C.-C.; Yee, N.; Barkay, T., Microbial transformations in the mercury cycle. In *Environmental Chemistry and Toxicology of Mercury*, Liu, G.; Cai, Y.; O'Driscoll, N., Eds. John Wiley & Sons, Inc.: 2012; pp 155-191.
2. Mason, R. P.; Choi, A. L.; Fitzgerald, W. F.; Hammerschmidt, C. R.; Lamborg, C. H.; Soerensen, A. L.; Sunderland, E. M., Mercury biogeochemical cycling in the ocean and policy implications. *Environ. Res.* **2012,** *119* (0), 101-117.
3. Soerensen, A. L.; Mason, R. P.; Balcom, P. H.; Sunderland, E. M., Drivers of Surface Ocean Mercury Concentrations and Air–Sea Exchange in the West Atlantic Ocean. *Environ. Sci. Technol.* **2013,** *47* (14), 7757-7765.
4. Kirk, J. L.; St. Louis, V. L.; Hintelmann, H.; Lehnherr, I.; Else, B.; Poissant, L., Methylated Mercury Species in Marine Waters of the Canadian High and Sub Arctic. *Environ. Sci. Technol.* **2008,** *42* (22), 8367-8373.
5. Malcolm, E. G.; Schaefer, J. K.; Ekstrom, E. B.; Tuit, C. B.; Jayakumar, A.; Park, H.; Ward, B. B.; Morel, F. M. M., Mercury methylation in oxygen deficient zones of the oceans: No evidence for the predominance of anaerobes. *Mar. Chem.* **2010,** *122* (1–4), 11-19.
6. Lehnherr, I.; St. Louis, V. L.; Hintelmann, H.; Kirk, J. L., Methylation of inorganic mercury in polar marine waters. *Nature Geosci* **2011,** *4* (5), 298-302.
7. Heimbürger, L.-E.; Cossa, D.; Marty, J.-C.; Migon, C.; Averty, B.; Dufour, A.; Ras, J., Methyl mercury distributions in relation to the presence of nano-and picophytoplankton in an oceanic water column (Ligurian Sea, North-western Mediterranean). *Geochim. et Cosmochim. Acta* **2010,** *74* (19), 5549-5559.
8. Watras, C. J.; Bloom, N. S., Mercury and methylmercury, in individual zooplankton: Implications for bioaccumulation. *Limnol. Oceanogr.* **1992,** *37* (6), 1313-1318.
9. Mason, R. P.; Reinfelder, J. R.; Morel, F. M. M., Uptake, Toxicity, and Trophic Transfer of Mercury in a Coastal Diatom. *Environ. Sci. Technol.* **1996,** *30* (6), 1835-1845.
10. Hammerschmidt, C. R.; Finiguerra, M. B.; Weller, R. L.; Fitzgerald, W. F., Methylmercury accumulation in plankton on the continental margin of the Northwest Atlantic Ocean. *Environ. Sci. Technol.* **2013,** *47* (8), 3671-3677.
11. Hammerschmidt, C. R.; Fitzgerald, W. F., Bioaccumulation and trophic transfer of methylmercury in Long Island Sound. *Arch. Environ. Contam. Toxicol.* **2006,** *51* (3), 416-424.
12. Hall, B. D.; Bodaly, R. A.; Fudge, R. J. P.; Rudd, J. W. M.; Rosenberg, D. M., Food as the Dominant Pathway of Methylmercury Uptake by Fish. *Water Air Soil Pollut.* **1997,** *100* (1-2), 13-24.
13. Wright, D. D.; Frazer, T. K.; Reinfelder, J. R., The influence of river plume dynamics on trace metal accumulation in calanoid copepods. *Limnol. Oceanogr.* **2010,** *55* (6), 2487-2502.
14. Kehrig, H. d. A., Mercury and Plankton in Tropical Marine Ecosystems: A Review. *Oecologia Australis* **2011,** *15* (4), 869-880.
15. Lehnherr, I.; St. Louis, V. L., Importance of Ultraviolet Radiation in the Photodemethylation of Methylmercury in Freshwater Ecosystems. *Environ. Sci. Technol.* **2009,** *43* (15), 5692-5698.

16. Monperrus, M.; Tessier, E.; Amouroux, D.; Leynaert, A.; Huonnic, P.; Donard, O. F. X., Mercury methylation, demethylation and reduction rates in coastal and marine surface waters of the Mediterranean Sea. *Mar. Chem.* **2007,** *107* (1), 49-63.
17. Hammerschmidt, C. R.; Bowman, K. L., Vertical methylmercury distribution in the subtropical North Pacific Ocean. *Mar. Chem.* **2012,** *132–133* (0), 77-82.
18. Whalin, L.; Kim, E.-H.; Mason, R., Factors influencing the oxidation, reduction, methylation and demethylation of mercury species in coastal waters. *Mar. Chem.* **2007,** *107* (3), 278-294.
19. Mason, R. P.; Lawson, N. M.; Sheu, G. R., Mercury in the Atlantic Ocean: factors controlling air–sea exchange of mercury and its distribution in the upper waters. *Deep Sea Res. Part 2 Top. Stud. Oceanogr.* **2001,** *48* (13), 2829-2853.
20. Soerensen, A. L.; Sunderland, E. M.; Holmes, C. D.; Jacob, D. J.; Yantosca, R. M.; Skov, H.; Christensen, J. H.; Strode, S. A.; Mason, R. P., An Improved Global Model for Air-Sea Exchange of Mercury: High Concentrations over the North Atlantic. *Environ. Sci. Technol.* **2010,** *44* (22), 8574-8580.
21. Mason, R. P.; Morel, F. M. M.; Hemond, H. F., The role of microorganisms in elemental mercury formation in natural waters. *Water Air Soil Poll.* **1995,** *80*, 775-787.
22. Lanzillotta, E.; Ceccarini, C.; Ferrara, R.; Dini, F.; Frontini, F. P.; Banchetti, R., Importance of the biogenic organic matter in photo-formation of dissolved gaseous mercury in a culture of the marine diatom Chaetoceros sp. *Sci. Total Environ.* **2004,** *318* (1–3), 211-221.
23. Wu, Y.; Wang, W.-X., Intracellular speciation and transformation of inorganic mercury in marine phytoplankton. *Aquat. Toxicol.* **2014,** *148* (0), 122-129.
24. Gregoire, D. S.; Poulain, A. J., A physiological role for Hg(II) during phototrophic growth. *Nature Geosci.* **2016,** *9* (2), 121-125.
25. Baeyens, W.; Leermakers, M., Elemental mercury concentrations and formation rates in the Scheldt estuary and the North Sea. *Mar. Chem.* **1998,** *60* (3–4), 257-266.
26. Senn, D. B.; Chesney, E. J.; Blum, J. D.; Bank, M. S.; Maage, A.; Shine, J. P., Stable Isotope (N, C, Hg) Study of Methylmercury Sources and Trophic Transfer in the Northern Gulf of Mexico. *Environ. Sci. Technol.* **2010,** *44* (5), 1630-1637.
27. Blum, J. D.; Popp, B. N.; Drazen, J. C.; Anela Choy, C.; Johnson, M. W., Methylmercury production below the mixed layer in the North Pacific Ocean. *Nature Geosci* **2013,** *6* (10), 879-884.
28. Kwon, S. Y.; Blum, J. D.; Chen, C. Y.; Meattey, D. E.; Mason, R. P., Mercury Isotope Study of Sources and Exposure Pathways of Methylmercury in Estuarine Food Webs in the Northeastern U.S. *Environ. Sci. Technol.* **2014,** *48* (17), 10089-10097.
29. Bergquist, B. A.; Blum, J. D., Mass-dependent and mass-independent fractionation of Hg isotopes by photo-reduction in aquatic systems. *Science* **2007,** *318* (5849), 417-420.
30. Zheng, W.; Hintelmann, H., Mercury isotope fractionation during photoreduction in natural water is controlled by its Hg/DOC ratio. *Geochim. Cosmochim. Acta* **2009,** *73* (22), 6704-6715.
31. Zheng, W.; Hintelmann, H., Isotope Fractionation of Mercury during Its Photochemical Reduction by Low-Molecular-Weight Organic Compounds. *J. Phys. Chem. A* **2010,** *114* (12), 4246-4253.

632 32. Ghosh, S.; Schauble, E. A.; Lacrampe Couloume, G.; Blum, J. D.; Bergquist, B. A.,
633 Estimation of nuclear volume dependent fractionation of mercury isotopes in equilibrium
634 liquid–vapor evaporation experiments. *Chem. Geol.* **2013,** *336* (0), 5-12.
635 33. Kritee, K.; Blum, J. D.; Johnson, M. W.; Bergquist, B. A.; Barkay, T., Mercury Stable
636 Isotope Fractionation during Reduction of Hg(II) to Hg(0) by Mercury Resistant
637 Microorganisms. *Environ. Sci. Technol.* **2007,** *41* (6), 1889-1895.
638 34. Kritee, K.; Barkay, T.; Blum, J. D., Mass dependent mercury stable isotope
639 fractionation during *mer* mediated microbial degradation of monomethylmercury. *Geochim.*
640 *Cosmochim. Acta* **2009,** *73* (5), 1285-1296.
641 35. Kritee, K.; Blum, J. D.; Barkay, T., Mercury stable isotope fractionation during
642 reduction of Hg(II) to Hg(0) by different microbial pathways. *Environ. Sci. Technol.* **2008,**
643 *42* (24), 9171-9177.
644 36. Rodriguez-Gonzalez, P.; Epov, V. N.; Bridou, R.; Tessier, E.; Guyoneaud, R.;
645 Monperrus, M.; Amouroux, D., Species-Specific Stable Isotope Fractionation of Mercury
646 during Hg(II) Methylation by an Anaerobic Bacteria (*Desulfobulbus propionicus*) under Dark
647 Conditions. *Environ. Sci. Technol.* **2009,** *43* (24), 9183-9188.
648 37. Perrot, V.; Bridou, R.; Pedrero, Z.; Guyoneaud, R.; Monperrus, M.; Amouroux, D.,
649 Identical Hg Isotope Mass Dependent Fractionation Signature during Methylation by Sulfate-
650 Reducing Bacteria in Sulfate and Sulfate-Free Environment. *Environ. Sci. Technol.* **2015,** *49*
651 (3), 1365-1373.
652 38. Kritee, K.; Blum, J. D.; Reinfelder, J. R.; Barkay, T., Microbial stable isotope
653 fractionation of mercury: A synthesis of present understanding and future directions. *Chem.*
654 *Geol.* **2013,** *336* (0), 13-25.
655 39. Price, N. M.; Harrison, G. I.; Hering, J. G.; Hudson, R. J.; Nirel, P. M.; Palenik, B.;
656 Morel, F. M., Preparation and chemistry of the artificial algal culture medium Aquil. *Biol.*
657 *Oceanogr.* **1989,** *6* (5-6), 443-461.
658 40. Zhong, H.; Wang, W.-X., Controls of Dissolved Organic Matter and Chloride on
659 Mercury Uptake by a Marine Diatom. *Environ. Sci. Technol.* **2009,** *43* (23), 8998-9003.
660 41. Morelli, E.; Ferrara, R.; Bellini, B.; Dini, F.; Di Giuseppe, G.; Fantozzi, L., Changes
661 in the non-protein thiol pool and production of dissolved gaseous mercury in the marine
662 diatom Thalassiosira weissflogii under mercury exposure. *Sci. Total Environ.* **2009,** *408* (2),
663 286-293.
664 42. Schaefer, J. K.; Morel, F. M. M., High methylation rates of mercury bound to
665 cysteine by Geobacter sulfurreducens. *Nature Geosci* **2009,** *2* (2), 123-126.
666 43. Parker, J. L.; Bloom, N. S., Preservation and storage techniques for low-level aqueous
667 mercury speciation. *Sci. Total Environ.* **2005,** *337*, 253– 263.
668 44. Amyot, M.; Gill, G. A.; Morel, F. M., Production and loss of dissolved gaseous
669 mercruy in coastal seawater. *Environ. Sci. Technol.* **1997,** *31*, 3606-3611.
670 45. Blum, J. D.; Johnson, M. W., Recent developments in mercury stable isotope
671 analysis. *Reviews in Mineralogy and Geochemistry* **2017,** *82* (1), 733-757.
672 46. Blum, J. D.; Bergquist, B. A., Reporting of variations in the natural isotopic
673 composition of mercury. *Anal. Bioanal. Chem.* **2007,** *388* (2), 353-359.
674 47. Sherman, L. S.; Blum, J. D.; Dvonch, J. T.; Gratz, L. E.; Landis, M. S., The use of Pb,
675 Sr, and Hg isotopes in Great Lakes precipitation as a tool for pollution source attribution. *Sci.*
676 *Total Environ.* **2015,** *502*, 362-374.

48. Aluwihare, L. I.; Repeta, D. J., A comparison of the chemical characteristics of oceanic DOM and extracellular DOM produced by marine algae. *Anglais* **1999,** *186* (186), 105-117.
49. Dupont, C. L.; Ahner, B. A., Effects of copper, cadmium, and zinc on the production and exudation of thiols by *Emiliania huxleyi*. *Limnol. Oceanogr.* **2005,** *50* (2), 508-515.
50. Carlson, C. A.; Hansell, D. A., DOM sources, sinks, reactivity and budgets. In *Biogeochemistry of marine dissolved organic matter*, 2nd edition ed.; Hansell, D. A.; Carlson, C. A., Eds. Academic Press.: 2015; pp 65–126.
51. Qureshi, A.; O'Driscoll, N. J.; MacLeod, M.; Neuhold, Y.-M.; Hungerbühler, K., Photoreactions of mercury in surface ocean water: gross reaction kinetics and possible pathways. *Environ. Sci. Technol.* **2009,** *44* (2), 644-649.
52. Janssen, S. E.; Johnson, M. W.; Blum, J. D.; Barkay, T.; Reinfelder, J. R., Separation of monomethylmercury from estuarine sediments for mercury isotope analysis. *Chem. Geol.* **2015,** *411*, 19-25.
53. Dupont, C. L.; Goepfert, T. J.; P. Lo; Wei, L. P.; Ahnerz, B. A., Diurnal cycling of glutathione in marine phytoplankton: Field and culture studies. *Limnol. Oceanogr.* **2004,** *49*, 991-996.
54. Satoh, M.; Hirachi, Y.; Yoshioka, A.; Kobayashi, M.; Oyama, Y., Determination of cellular levels of nonprotein thiols in phytoplankton and their correlations with susceptibility to mercury. *J. Phycol.* **2002,** *38* (5), 983-990.
55. Kawakami, S. K.; Gledhill, M.; Achterberg, E. P., Production of phytochelatins and glutathione by marine phytoplankton in response to metal stress. *J. Phycol.* **2006,** *42* (5), 975-989.
56. Wu, Y.; Wang, W.-X., Accumulation, subcellular distribution and toxicity of inorganic mercury and methylmercury in marine phytoplankton. *Environmental Pollution* **2011,** *159* (10), 3097-3105.
57. Zhang, T.; Hsu-Kim, H., Photolytic degradation of methylmercury enhanced by binding to natural organic ligands. *Nat. Geosci.* **2010,** *3*, 473-476.
58. Liu, Y.; Edge, R.; Henbest, K.; Timmel, C. R.; Hore, P. J.; Gast, P., Magnetic field effect on singlet oxygen production in a biochemical system. *Chem. Comm.* **2005,** (2), 174-176.
59. Pinto, E.; Sigaud-kutner, T. C. S.; Leitao, M. A. S.; Okamoto, O. K.; Morse, D.; Colepicolo, P., Heavy metal induced oxidative stress in algae. *J. Phycol.* **2003,** *39* (6), 1008-1018.
60. Laws, E. A.; Letelier, R. M.; Karl, D. M., Estimating the compensation irradiance in the ocean: The importance of accounting for non-photosynthetic uptake of inorganic carbon. *Deep Sea Res. Part 1 Oceanogr. Res. Pap.* **2014,** *93*, 35-40.